IMPACT OF CELLULOSE FILAMENTS ON INTERLAMINAR PROPERTIES, FLAMMABILITY AND THERMAL DEGRADATION BEHAVIOUR OF POLYMER MATRIX COMPOSITES

F. Lessard[1], C. Boanta[1], M. Dubé[2], L. Laberge-Lebel, and É. Robert*

[1]Department of Mechanical Engineering, École Polytechnique Montréal, Montréal, Canada
[2]Department of Mechanical Engineering, École de technologie supérieure, Montréal, Canada
[3]High Performance Polymer and Composite Systems (CREPEC), Polytechnique Montreal
*É. Robert (etienne.robert@polymtl.ca)

Keywords: Hybrid Composite, Cellulose fibre, Aerospace, Interlaminar Strength

ABSTRACT

A fibre reinforced thermoplastic composite material composed of polyamide 6 with fire-retardant additive (PA6-FR), glass fibre, and cellulose fibre was tested for application in aircraft cabin interior. Literature suggests the addition of cellulose fibre improves interlaminar properties of thermoset composite materials yet, very little was published on thermoplastic composites. Plates samples were manufactured using this material to measure the impact of cellulose fibre addition on interlaminar and flammability properties, the latter being of crucial importance for aircraft interior applications. This material was then benchmarked against PA6 and PA66 without fire-retardant additive. While the addition of cellulose fibre did not achieve the targeted improvement of interlaminar shear strength, it highlighted an unexpected flame-retardant behaviour of the cellulose fibre.

1 INTRODUCTION

Nanocellulose, a nanoparticle extracted from wood, offers a unique opportunity to introduce bio-sourced fibre material in demanding environments such as the aeronautical industry. Nanocellulose is an engineered material - as it is extracted from natural fibres - demonstrating predictable and repeatable properties, unlike other conventional plant-derived fibres [1]. Specifically, cellulose nanoparticles such as cellulose nanofibrils (CNF) exhibit high tensile strength and have lately been used to increase interfacial and interlaminar strength in polymer matrix composites (PMCs) [2, 3].

Despite the positive contribution of natural fibres to the mechanical properties of PMCs, their high flammability is of concern in aircraft interior applications in the event of an accidental fire [4]. The decomposition temperature of such natural fibres is low, typically around 200°C, which results in the outgassing of combustible volatile species [5]. In addition, their high oxygen content may lead to a decrease in the overall limiting oxygen index (LOI) of the PMC, effectively decreasing its fire retardant properties. However, natural fibres are known to produce char upon combustion [6], which provides a protective layer to the virgin polymer matrix further from the flame [7]. This layer limits the heat transfer and the molecular diffusion of oxidative species in the virgin phase, thus slowing further decomposition [4].

The work presented here investigates the potential of CNF addition to a polymer resin in the context of application to aircraft interiors. This application requires high specific material properties to reduce aircraft weight while imposing stringent criteria on flame, smoke, and toxicity (FST) of the composite upon combustion.

2 MATERIALS

A fire-retardant polyamide-6 (PA6-FR) polymer was used in this study; the selected product, *Ultramid B3U Q721* was provided by BASF and is already certified to be compliant with FAR 25.853 regulations. *Kruger Biomaterials* kindly provided the cellulose fibres (CF) used in this study. The cellulose fibres used in this study (FiloCell, *Kruger Biomaterials*) have a density of 1450 kg/m^3, a length of 100-2000 µm, and a diameter of 80-300 nm. The cellulose fibres were compounded with the PA6-FR by *Kruger Biomaterials* using a twin-screw extruder to produce film with a nominal thickness of

100 µm. The film's cellulose fibre content was approximately 4-wt%. Glass fibre single-end roving (SE1200, 735 tex, Owens Corning) was used to produce composite plates by a film-stacking method described below. Films made of virgin (without cellulose fibres) PA6-FR are extruded in-house using a twin screw extruder (ZSE 18HP, *Leistritz*). Films of neat polyamide (6400 series, PA66, 50 µm film, *KNF Flexpak*) are used as a baseline as well as glass fibre commingled fibre (GF/PA6, 50%Vf, *Concordia Fibers*). Neat polyamide-66 films are used to assess the influence of fire-retardant particles while PA6 commingled fibers are used to evaluate the effect of film-stacking process on the properties of the laminates produced.

3 METHODOLOGY

3.1 Compression moulding

Composite samples are manufactured by compression moulding using a film stacking technique. A custom apparatus, similar to a filament winding machine, is used to wind fibre on a preforming frame alternated by film of polymers until the target stackup is achieved (figure 1a). Samples are then moulded using a preforming frame and steel mould illustrated in figure 1b. The mould produces plates of 305x355 mm^2, with thicknesses up to 6mm. Preforms are dried for 12h at 80°C in an oven prior to moulding. The preform is placed in the mould and a 100 ton hydraulic press (Accudyne) equipped with heated platens is used to heat and consolidate the sample (figure 1b). The pressure and temperature cycle is illustrated in figure 1c. An initially light pressure is applied to insure adequate contact between the press' platens and the mould during preheating. Once the processing temperature of 260°C is attained, pressure is gradually increased by steps of 0.6 MPa until a full pressure of 2 MPa is reached, and then held for 10 min. Cooling is then started and the pressure maintained until the temperature is below the glass transition temperature (60°C). A thermocouple (Type J, 30AWG) is used to measure the internal sample temperature along the cycle. Initial testing revealed a higher then expected void content in samples produced. This problem is solved by using a vacuum bag to remove air and help compress the preform. It also adds the benefit of reducing PA6 melt oxidation since nitrogen blanketing is not available in the equipment.

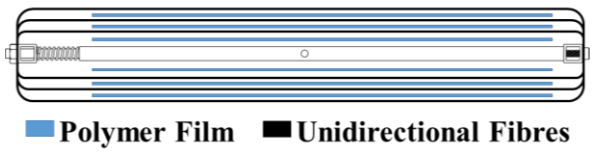

(a)

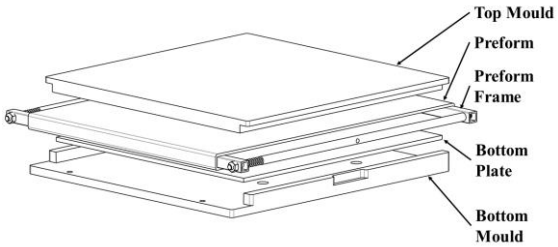

(b)

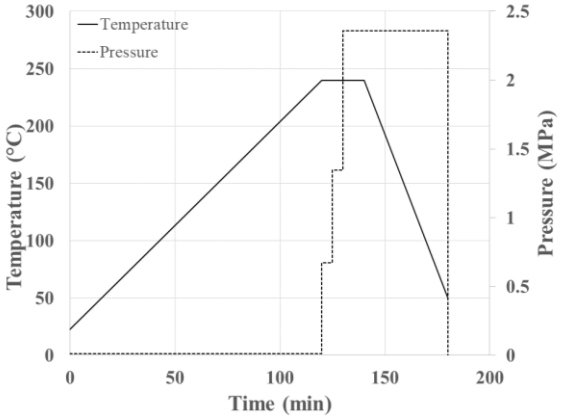

(c)

Figure 1: (a) Schematic of a preform illustrating the film stacking methodology (b) Schematic of mould for plate manufacturing (c)Temperature and pressure during manufacturing cycle

Samples made of commingled fibres and PA6-FR were manufactured first and rather high fibre volume fractions were obtained. However, the same volume fraction could not be obtained in samples containing cellulose fibres and neat PA66 polymer. For this reason, a second sample was produced with a reduced fibre content.

3.2 Thermogravimetry

The thermogravimetric analysis (TGA) is performed in a TA Instruments Q500 thermogravimetric analyzer. Each composite constituent is tested once in each type of atmosphere, namely an inert atmosphere (N_2) and an oxidative atmosphere (N_2+O_2), with a sample purge flow of 20 mL/min. Prior to the TGA experiments, the samples have been dried in a vacuum of 22 inHg at a temperature of 105ºC for 12h. The individual test samples include cellulose filaments (CF), commingled polyamide-6 with glass fibre strands (PA6/GF), fire-retardant polyamide-6 film (PA6-FR) and fire-retardant polyamide-6 film with 2 wt% cellulose filaments (PA6-FR/CF), glass-fibre-reinforced polyamide-6 composite (PA6/GF) and fire-retardant polyamide-6 with cellulose filaments and glass fibre reinforcement (PA6-FR/CF/GF). The test specimens are placed in a platinum crucible (*DSC Consumables*) and subjected to a temperature ramp of 10ºC/min from ambient temperature until 700ºC, followed by an isothermal of 10 min. at 700ºC. The furnace temperature is then brought down to 30ºC prior to the removal of the crucible.

3.3 Composite Constituents Measurement

Evaluation of constituent volumetric fraction is done through pyrolysis of the samples according to ASTM D3171. The density of the samples is measured in hexadecane using an analytical scale and density apparatus (*Sartorius LA and YDK-01*). Samples are then pyrolyzed in an oven at 565°C for 1 hour. Pyrolysis of samples of PA6-FR and glass fibres alone was performed to validate that no residue is left after matrix burnout and that fibre mass is not affected by the process. Density of the fibres is measured with a gas pycnometer over 10 samples. Since polyamides are semi-crystalline polymers, density changes depending on sample crystallinity. DSC measurements (TA Instruments Q2000) are performed to evaluate the crystalline fraction of samples produced.

3.4 Interlaminar Shear Strength Measurement

The interlaminar shear strength (ILSS) of the samples produced is measured through a short beam shear test interpreted from ASTM D2344. Specimen are first cut using a tile saw equipped with a diamond blade. Plates produced have a nominal thickness of 5mm therefore samples are cut to dimensions of 10x30mm as to follow the ASTM's guidelines. The mechanical testing apparatus available consists of a 3-point bending jig with a nose radius of 10mm which differs from ASTM D2344

(which states a 3 mm radius for supports). Specimens are conditioned at room temperature and relative humidity for 24h before testing.

3.5 Implementation of FAA Fire Testing Handbook Chap 1 tests

The flammability experiments are carried out in a closed cabinet designed according to the FAA Material Fire Test Handbook (FAA-MFTH). The cabinet is equipped with a fume hood connected to a ventilation system. Care has been taken to ensure that the ventilation flow rate does not disturb the flame. The test specimens of size 305 x 75mm and various thicknesses are conditioned in a 22 inHg vacuum for 12h and another 24h at room temperature and 25% relative humidity. The test specimens are weighed and then clamped vertically in the specimen holder. The tests are performed under the conditions specified in Chapter 1 of the FAA-MFTH [8]. The burner is operated in the premixed configuration using methane as the fuel (purity of 99.0%) and ambient air as the oxidizer. The fuel supply pressure is set at 2.5 psi, resulting in a flow rate of approximately 0.9 SPLM. The air intake of the burner is adjusted to yield a flame composed of a 22 mm-high inner cone and an overall flame height of 38 mm, as per the FAA-MFTH. The location of the burner relative to the specimen is such that the tip of the inner flame cone coincides with the front-bottom edge of the test specimen. Each flammability test consists of subjecting the test specimen to the flame for 60 seconds, after which, the flame is removed; this parameter is termed ‘’ignition time’’. The test specimens are allowed to continue burning if sustained combustion occurs and the duration of sustained combustion is recorded as the ‘’flame time’’. Throughout the duration of the test, burning drips are counted and the duration of sustained combustion of drips is measured and termed ‘’drip flame time’’. When combustion of the test specimen stops, the specimen is removed from the specimen holder and weighed. In addition, the burn length is measured along the specimen’s longitudinal axis from the edge subjected to the flame. The burn length only includes the region where obvious degradation occurred (partial consumption, charring or embrittlement); sooty, shrunk, melted, discolored and warped regions are not included.

4 RESULTS

4.1 Composite Constituents Measurement

DSC measurements of polyamides composite samples revealed the absence of a cold crystallization peak during initial heating. Figure 2 illustrates a typical heating cycle in a DSC at 10°C/min from 0 to 260°C. Fusion enthalpy was measured for 4 samples. 100% crystalline polyamide 6 fusion enthalpy was taken as 230 J/g [9]. The crystallinity fraction was found following the equation below, where ΔH_m is the measured fusion enthalpy, ΔH_c the cold crystallisation enthalpy, ΔH_f the theoretical enthalpy for 100% crystallinity, and m_f the composite fibre mass fraction. Average crystallinity was found to be around 30%. This result is coherent with the slow cooling rates imposed (~10°C/min) during samples manufacturing.

$$\%X = \frac{\Delta H_m + \Delta H_c}{\Delta H_f(1 - m_f)}$$

An identical thermal cycle was imposed to neat polymer samples using an oven before measuring density using the same method. The density of the PA6-FR polymer was measured as 1167 kg/m^3 and the PA66 film 1122 kg/m^3, which is in agreement with the datasheet values given by the manufacturers. Density measurement of glass fibres, done through a gas pycnometer, revealed a density of 2651 kg/m^3 for Owens Corning product and 1935 kg/m^3 which is also coherent with datasheet values. The volume fractions of samples’ constituents are presented in table 1 below. Fibre and void content are presented in volumetric fraction, respectively as V_f and V_v for samples used in mechanical tests. Samples intended for flammability test have their glass fibre content expressed in mass fraction. Notice that only high volumetric fibre contents were tested for flammability. Figure 3 illustrates a typical micrography of a mechanical test coupon cross section where a small amount of void is visible.

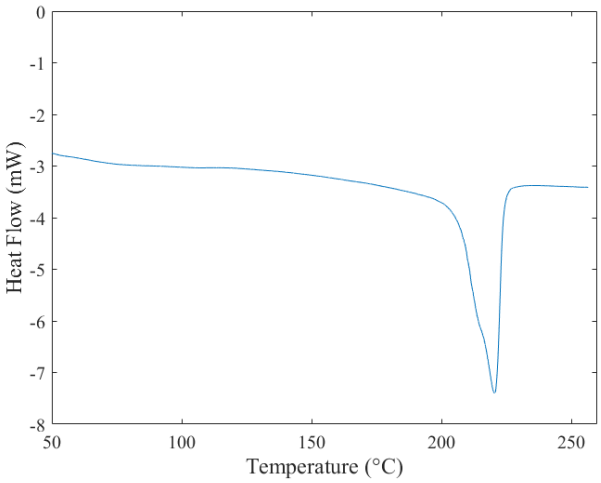

Figure 2: Typical response during DSC testing of polyamide composite samples.

System	Mechanical Test			Flammability Test		
	V_f	V_v	V_{CF}	m_f	V_v	m_{CF}
PA6-FR 60Vf	62 ± 1	1.3 ± 0.4	-	76 ± 4	0.6 ± 0.2	-
PA6-FR 40Vf	37 ± 1	1.0 ± 0.5	-	-	-	-
PA6-FR+CF	40 ± 2	0.2 ± 0.1	1.95*	70	n/a	1.61*
PA66 Film	40 ± 5	0.9 ± 0.8	-	68 ± 3	1.6 ± 0.7	-
PA6 Commingled	59 ± 1	1.9 ± 0.6	-	77 ± 2	1.3	-

*Estimated

Table 1: Constituent as measured in samples for mechanical and flammability tests

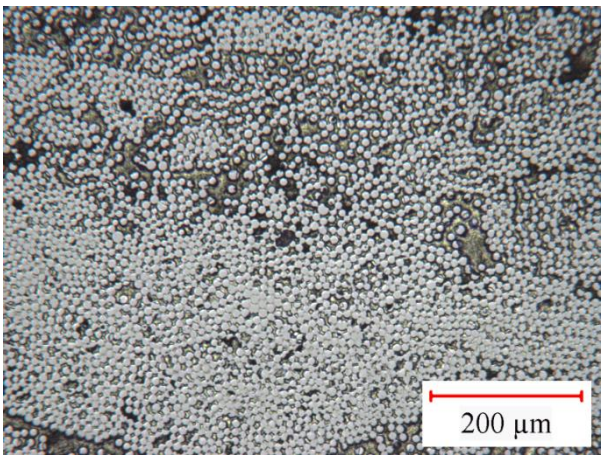

Figure 3: Typical micrography of a sample produced using PA6-FR and glass fibre (x100 magnification)

4.2 Interlaminar Shear Strength Measurement

The interlaminar shear stress is given by the equation below where σ is the interlaminar shear stress (MPa), P is the force applied (N), *w* the sample width (mm), and *t* its thickness (mm). The interlaminar shear strength is obtained with the same equation using the maximum load supported by the sample. In the following figure 4, the stress is plotted against the displacement normalized by the sample thickness.

Figures 4(a) through (e) illustrate mechanical behaviour of each specimen tested. Each curve is associated with a sample. As can be seen, specimens demonstrate relatively low variability at low strains (0-5%) but as the stress grows closer to the maximum, the stiffness changes. This phenomenon is likely due to damage accumulation in the sample as stress/displacement curve becomes non-linear. Figure 4(f) illustrates the average response and the standard deviation as a shaded zone for each material. The standard deviation is small (~2MPa) on the initial slope and up to the maximum stress. After the onset of failure, the deviation grows larger (>5MPa) since the failure of each sample test is almost random. From this figure, it can also be observed that the rigidity is affected by the fibre content: Samples with higher glass fibre content (PA66-FR 60Vf and PA6 Commingled) exhibit a stiffer response than samples with lower glass fibre content. For the three samples produced by film stacking with a fibre fraction of ~40% (PA6-FR 40Vf, PA6-FR+CF, PA66 Film), the initial stiffness is similar but quickly diverges. Samples containing cellulose fibres (PA6-FR+CF) exhibit the lowest stiffness while samples made of PA66 films (PA66 Film) exhibit the highest stiffness of the three. Samples with higher fibre volume fraction (PA66-FR 60Vf, PA6 Commingled) also exhibit a more abrupt rupture once the maximum stress is reached. In samples PA6-FR 40Vf, PA6-FR+CF, and PA66 Film, the stress rise is linear up to 5% or less normalized displacement. After this point, the stress rise is non-linearly reducing until it reaches a plateau. This pseudo-ductile behaviour is consistent with damage accumulation. Samples using the fire-retardant polymer display a reduction in stress of approximately 10% after the onset of failure while samples using neat polymer films (PA66 Film) maintains a relatively constant stress. This suggests a higher amount of energy absorption.

$$\sigma = \frac{3}{4}\frac{P}{w\,t}$$

Table 2 contains the average interlaminar shear strength (ILSS) measured for the different specimens. The variation in the number of samples reported (n) is due to samples being rejected for reasons such as incorrect failure mode or statistical outliers (Grubb's test). The specimens manufactured from commingled fibres and film staking using virgin polyamide (PA66 Film) display significantly higher ILSS than the ones made out of the fire-retardant grade. Of those, samples with higher fibre volume fraction exhibit the lowest strength. This behaviour is somewhat unexpected since literature published on carbon epoxy laminates [10] suggests that higher fibre fraction correlates with higher ILSS. This loss in strength is suspected, in this case, to be caused by an interaction with the fire-retardant additive as similar performance to PA66 film stacked samples was expected. The specific fire-retardant additive used in *Ultramid B3U* is melamine cyanurate (*Melapur MC*, BASF), with an average particle size close to the glass fibre's diameter used in this study. Further investigations would be required to determine the specific mechanism of this interaction. Finally, the presence of cellulose fibres affected negatively the strength and stiffness of the samples tested compared to samples with similar fibre fraction (PA6-FR 40Vf, PA6-FR+CF). However, a slight (14%) but statistically significant (T-Test, $n_1=8$, $n_2=9$, $\mu_1=28.5$, $\mu_2=33.4$, $\sigma_1=10.7$, $\sigma_2=4.1$, $p<0.05$) increase is seen with the sample at higher fibre faction (PA6-FR 60Vf, PA6-FR+CF). Again, the specific mechanism behind these results is unknown and would require further study.

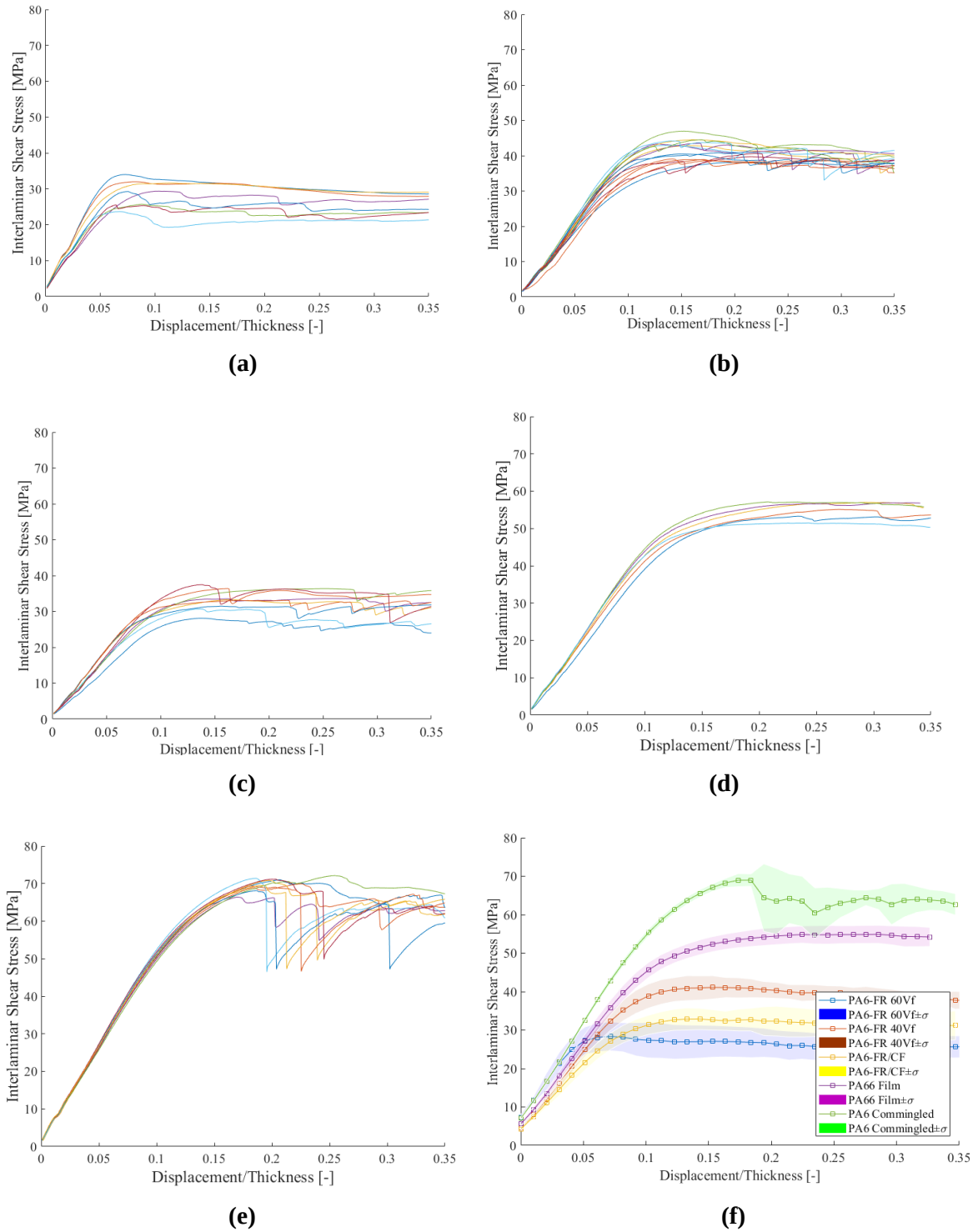

Figure 4: Mechanical behaviour during short beam shear test for material (a)PA6-FR 60Vf, (b)PA6-FR 40Vf, (c)PA6-FR+CF (40%Vf), (d)PA66 Film (40%Vf), (e)PA6 Commingled (59%Vf), and (f) all material combined with standard deviation

System	ILSS (MPa)	n
PA6-FR 60Vf	29 ± 3	8
PA6-FR 40Vf	42 ± 3	16
PA6-FR+CF	33 ± 2	9
PA66 Film	53 ± 5	6
PA6 Commingled	70 ± 1	9

Table 2: Interlaminar shear strength with standard deviation and number of sample tested

4.3 Thermogravimetry

4.3.1 Inert atmosphere

The thermogravimetric mass loss (TGA curves) and mass loss rate (DTG curves) obtained in an inert atmosphere for the composite constituents are shown in Fig. 5 and 6, respectively. The cellulose filaments exhibit a slow and monotonic weight loss from the beginning of the temperature ramp until around 220°C, at which point 2.5 wt% is lost. This observation is associated with the progressive dehydration of the cellulose fibres. Starting at 220°C, the weight loss rate becomes very steep and upon reaching 445°C, 93.5 wt% of the weight is lost. The bulk of the mass loss is associated with the outgassing of H_2, CO, CO_2 and CH_4 and other organics occurring at temperatures around 380°C, as indicated by Yang [5]. From 445°C until 700°C, the weight loss reverts to slow and monotonic, stagnating around 595°C. A considerable amount of residue (ca. 7 wt%) remains from the thermal degradation of cellulose, possibly associated with an enhanced char formation due to the inert atmosphere. With regards to the thermal degradation of the fire-retardant polyamide-6 film (PA6-FR), it exhibits a monotonic weight loss at the beginning of the temperature ramp, similar to that of the raw cellulose filaments. However, upon reaching 270°C, the weight loss rate becomes significant up to a temperature of 500°C, after which the weight loss is negligible. The TGA curve of PA6-FR shows a two-stage degradation with a shoulder at 345°C. This observation may be explained by the respective degradation of the fire-retardant (10% weight loss), followed by the degradation of the resin. In fact, from the datasheet of the proprietary PA6-FR polymer, the fire-retardant content of the polymer is of the order of 10-15 wt% melamine cyanurate, which matches with the relative mass loss observed. When comparing the TGA curves of PA6-FR and PA6/GF, there seems to be a synergistic degradation reaction between the PA6 polymer and the fire-retardant. The degradation of PA6 in the PA6-FR film onsets at 345°C whereas that of PA6 in the PA6/GF composite onsets around 360°C. A TGA analysis of commingled PA6/GF fibres confirms this observation but is not shown in the plot. This observation is consistent with the mode of action of melamine cyanurate in aliphatic polyamides, which promotes char formation at the expense of thermal stability [11]. The thermal degradation behaviour of the PA6-FR/CF film is similar to that of the PA6-FR. Considering the low CF mass loading in this film, such an observation is expected. Nevertheless, a slight shift towards a higher temperature can be observed at the peak mass loss rate for the PA6-FR/CF film with respect to that of the PA6/FR in their respective DTG curves. This observation is most probably owed to the presence of cellulose. Indeed, DSC analysis of cellulose [5, 12] exhibits an endothermic peak at temperatures nearing 350°C, possibly explaining the observed delay in the degradation of the cellulose-reinforced composite. According to Ball et al. [13], the endothermic peak in the thermal degradation of cellulose is associated with a high activation energy volatilization process. Additionally, the resulting char acts as a protective shield, potentially delaying the degradation of the PA6 resin. With respect to the degradation of PA6-FR/CF/GF, it is possible to observe the mass loss associated to the fire retardant as well as that of the resin but the cellulose mass loss is not noticeable, possibly due to its low mass concentration in the composite. Additionally, mass

loss continues slowly in the high end of the temperature range (i.e. 490-650°C) for the PA6-FR/CF/GF composite.

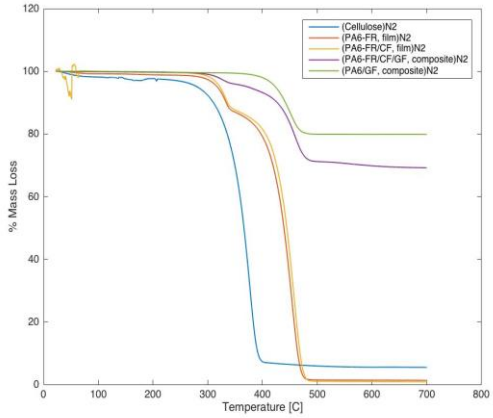

Figure 5: TGA plot of composite constituents in inert atmosphere

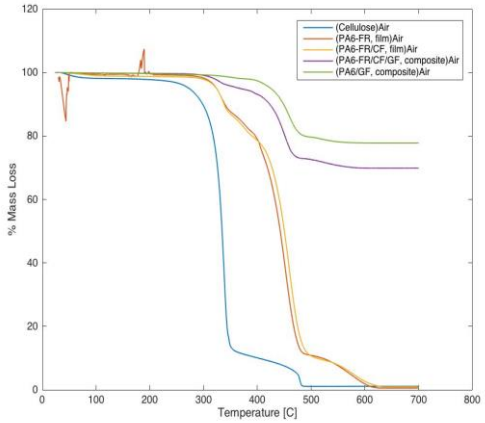

Figure 7: TGA plot of composite constituents in oxidative atmosphere

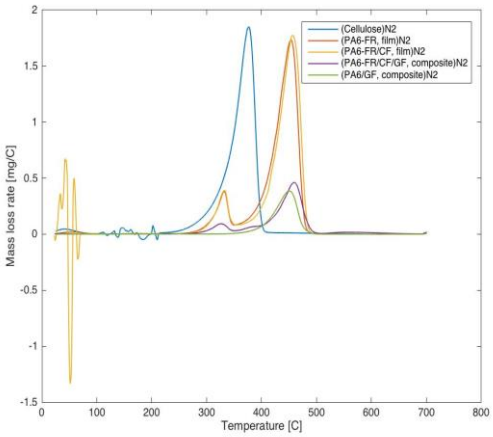

Figure 6: DTG plot of composite constituents in inert atmosphere

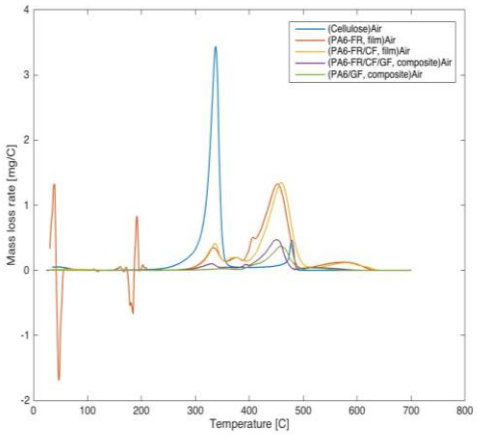

Figure 8: DTG plot of composite constituents in oxidative atmosphere

4.3.2 Oxidative atmosphere

The thermogravimetric mass loss (TGA curves) and mass loss rate (DTG curves) obtained in an oxidative atmosphere for the composite constituents are shown in Fig. 7 and 8, respectively. In this case, the degradation of cellulose occurs in three steps; the first represents the dehydration of the cellulose fibres while the second peak accounts for the pyrolysis and outgassing of volatiles starting at approximately 338°C. The third peak may be associated with the oxidation of char, considering the relatively high temperature of 475°C. The thermal degradation of the PA6-FR and PA6-FR/CF films exhibit the same peaks as in the inert atmosphere, with degradation stages around the same temperatures. In comparison to the inert atmosphere, additional but less significant peaks are observed for the PA6-FR systems in oxidative atmosphere around 400°C. Gijsman et al. [14] observed the emission of H_2, CO, CO_2, CH_4 and C_2, C_3, C_4 hydrocarbons upon the thermal degradation of PA6 with 10 wt% MC in an autoclave at 400°C and 450°C for 1h and 0.5h, respectively. The observed mass loss peaks at these temperatures may be associated with the outgassing of the above-mentioned species. Another degradation peak can be observed for both types of samples around 575°C in an oxidative atmosphere, we suspect that it is explained by the oxidation of char resulting from the polymer degradation. In addition, a sensibly larger delay (8°C) between the main degradation peaks of PA6-FR and PA6-FR/CF can be observed in oxidative atmosphere. An interesting observation regarding the PA6-FR/CF/GF composite is that in an oxidative atmosphere, the PA6 degradation peak occurs at a lower temperature

than the degradation of PA6 in the PA6/GF composite. It is suspected that the voids formed upon the degradation of cellulose increase the surface area of PA6 capable of reacting, thus promoting its more premature degradation in comparison to the degradation of PA6 in the PA6/GF composite.

4.4 FAA Fire Testing Handbook Chap 1 tests

The specimens tested for flammability are part of three different material systems, namely PA6/GF, PA6-FR/GF and PA6-FR/CF/GF. All the specimens tested burn throughout the entire exposed vertical distance of 285mm and no drips occur, thus the drip time of all specimens is 0 seconds. Since the burn length is longer than 152mm and the flame time is above 15 seconds for the 60-second ignition time applied here, all samples fail according to the FAA-MFTH criteria.

To reveal trends in the flame time, this value was plotted as a function of the percent weight loss but also as a function of the specimen thickness. These plots are not shown here, but the flame time does not exhibit any clear trend with respect to the percent weight loss for any of the three systems. This observation indicates that the fraction of combustible material in a specimen does not have a strong influence on the flame time, at least not in the experimental configuration exploited in this work. In fact, the rate at which a flame progresses through a material depends on the ability of the flame to preheat and pyrolyze the material to yield combustible species, which in turn mainly depends on the heat capacity and thermal conductivity of the virgin phase but also on the energy balance between the heat of combustion of the outgassing and the energy required for pyrolysis/gasification reactions. The ability of oxygen to diffuse to the region where outgassing of pyrolysates occurs is also relevant. In the configuration investigated here, the vertical specimen orientation means that buoyancy effect entrains the hot burned gases upwards towards the virgin regions of the specimen, effectively promoting the decomposition of the material. However, the presence of these gases also prevents the oxygen from penetrating readily to the pyrolysate outgas region. Without a constant supply of oxygen, the pyrolysis gases can escape without burning or burn well away from the sample, resulting in a mass loss without promoting the propagation of the flame through a heat feedback loop. As a result of this proposed mechanism, the relationship between the mass loss and the flame time is closely coupled with fluid mechanics parameters that cannot be quantified with the FAA testing cabined used here, hence the lack of direct correlation between these two parameters.

For each specimen, two thickness measurements have been made; one at the top and one at the bottom of the specimen, from which an average thickness is calculated. The flame spread results reveal that the flame time scales linearly with the specimen thickness, for all three systems. The linear relationship can then serve to normalize the flame time by the thickness of the specimens, thus allowing comparison between the different systems. In table 3, an equivalent flame time is computed for all specimens as if they had a thickness of 1mm. We suspect that this relationship is caused by the bulk of the combustion occurring at the base of the flame, across the thickness. In fact, at this location, the flame consumes the material more efficiently because oxygen is readily drawn in the flame from below by the convective mass transfer resulting from the buoyancy of the combustion products, as explained above. As such, the consumption of the combustible material across the thickness governs the rate at which the flame propagates.

The results shown in Table 3 indicate that the PA6-FR system would need 133 seconds to burn entirely if it had a 1 mm thickness, whereas the PA6 and PA6-FR/CF would require around 190 seconds. Surprisingly, the PA6-FR system would burn through a slab of 285x50x1 mm^3 (normalized exposed volume of the specimen in the FAA-MFTH-Chap.1) faster than the non-fire-retardant system (PA6) or the fire-retardant system which includes cellulose filaments (PA6/CF). The fire retardant used in the proprietary formulation is melamine cyanurate at a concentration of 10-15 wt% and it is known to have a worst performance as a fire-retardant in PA6 as compared to PA66 [14]. However, this fact does not justify its poor performance when compared to the other two systems which do not include any fire-retardant and further investigation of the fire retardant mode of action would be needed to explain this observation. Interestingly, the analysis involving the thickness-normalized flame time correlates well with the TGA results discussed above. The thermal degradation of PA6-FR/CF film in nitrogen

atmosphere occurs at a higher temperature than the degradation of the PA6-FR, which explains the longer time required for the PA6-FR/CF/GF system to burn entirely. In addition, the comparison of the flammability results for these systems is pertinent with the TGA data in the inert atmosphere because thermal degradation in the solid material occurs without atmospheric oxygen. As a result of the thermal degradation, pyrolysis gases are supplied and can mix with atmospheric oxygen at the base of the flame and participate in the heat feedback loop to promote further degradation of the virgin phase. In light of the above analysis, the degradation rate of the virgin phase is then a limiting step in the propagation of the flame and thus, it directly affects the flame time.

System	# of samples	Average system thickness (mm)	σ thickness (mm)	% Weight loss	Average system flame time (s)	σ flame time (s)	Thickness-normalized system flame time (s)
PA6 (P66*) /GF	3(2*)	1.64	0.36	14.9	306	73	187
PA6-FR	6	1.19	0.21	13.5	159	34	133
PA6-FR+CF	4	0.83	0.16	17.5	154	41	189

Table 3: Flammability results from the three material systems of PA6(PA66*) and glass fibre

This comparison using the normalized thickness must be used with caution as it assumes that the linear behaviour of each system extends to a thickness of 1mm. For the PA6/GF and PA6-FR/CF/GF systems, such a normalization represents an extrapolation of the data, as the thickness ranges considered for these two systems are above and below 1mm, respectively. Nevertheless, previous research on PMMA specimens has shown that the downward flame spread rate scales with the thickness, for sample thicknesses in the range of 1.5 mm to 10 mm [15], with the flame spread rate being an exponentially decaying function of the sample thickness. For the narrow thickness range explored in our work, the exponential decay function can be assumed as linear without drastically affecting the results. The flammability results compared through the thickness-normalized flame time reveal that the addition of ca. 1.61 wt% of cellulose filaments did not affect negatively this combustion parameter in fire-retardant PA6-glass fibre composites.

5 CONCLUSIONS

The material studied is not, in its current form, suitable for the targeted application. However, interesting findings open the door to further research on this material. Firstly, the enhancement of interlaminar strength, as suggested by other literature publications, was not observed. This may be due to a plethora of causes such as an inappropriate cellulose content, cellulose-polyamide poor adhesion, or even an interaction with the fire-retardant additive. Further studies are required to validate the cause of the phenomena observed.

Secondly, interesting combustion behaviour was observed in the material produced and correlations indicate a way forward to improve the fire performance of the material. Indeed, future tests will be performed with higher cellulose fractions since its presence has hinted towards a fire-retardant effect through enhanced char formation. Moreover, in addition to continuous glass fibres, systems with woven glass fibres will be investigated at different mass fractions as the continuity of the fibre result in an inert medium for heat storage and heat conduction different than what short glass fibres provide. In addition, larger sample thicknesses will be explored as it is expected that at a threshold thickness for a specific material system, the flame propagation will arrest readily after the removal of the ignition flame.

ACKNOWLEDGEMENTS

This project is part of the project COMP-1633 - Flame retardant FRP systems for aircraft interior applications and the help of the following partners: CRIAQ, Mitacs, German Federal Ministry of

Education and Research (BMBF), Kruger Biomaterials, Pultrusion Technique Inc., CompriseTec GmbH, Exakt Advanced Technologies GmbH, and Polytechnique Montréal, École de technologie supérieure (ETS), Helmut-Schmidt University (HSU), Technical University of Hamburg (TUHH).

REFERENCES

[1] Faruk, O., et al., *Biocomposites reinforced with natural fibers: 2000–2010.* Progress in polymer science, 2012. **37**(11): p. 1552-1596.

[2] Dufresne, A., *Nanocellulose: from nature to high performance tailored materials*. 2017: Walter de Gruyter GmbH & Co KG.

[3] Goswami, J., R.J. Moon, and K. Kalaitzidou. *Effect of Nanocellulose on the Properties of Glass Fiber/Nanocellulose/Unsaturated Polyester Resin Composites*. in *Proceedings of the American Society for Composites—Thirty-second Technical Conference*. 2017.

[4] Saba, N., et al, *A review on flammability of epoxy polymer, cellulosic and non-cellulosic fiber reinforced epoxy composites.* Polymers for Advanced Technologies, 2016. 27(5): p. 577-590.

[5] Yang, H., et al, *Characteristics of hemicellulose, cellulose and lignin pyrolysis.* Fuel, 2007. 86(12): p. 1781-1788.

[6] Sekiguchi, Y., J.S. Frye, and F. Shafizadeh, *Structure and formation of cellulosic chars.* Journal of Applied Polymer Science, 1983. 28(11): p. 3513-3525.

[7] Duquesne, S., et al., *Intumescent paints: fire protective coatings for metallic substrates.* Surface and Coatings Technology, 2004. 180-181: p. 302-307.

[8] Horner, A., *Chapter 1 Vertical Bunsen Burner Test for Cabin and Cargo Compartment Materials*, in *Aircraft Materials Fire Test Handbook*. 2000, U.S. Department of Transportation: Washington DC. p. 1-1 1-7.

[9] Blaine, R. L. (n.d.). Thermal Application Note - Polymer Heats of Fusion. Retrieved from http://www.tainstruments.com/pdf/literature/TN048.pdf

[10] Bowles, K. J., & Frimpong, S. (1992). Void Effects on the Interlaminar Shear Strength of Unidirectional Graphite-Fiber-Reinforced Composites. Journal of Composite Materials, 26(10), 1487–1509. https://doi.org/10.1177/002199839202601006

[11] Joseph, P. and J. Ebdon, Recent developments in flame-retarding thermoplastics and thermosets. 2001. p. 220-263.

[12] Wielage, B., et al., *Thermogravimetric and differential scanning calorimetric analysis of natural fibres and polypropylene.* Thermochimica Acta, 1999. **337**(1-2): p. 169-177.

[13] Ball, R., A.C. McIntosh, and J. Brindley, Feedback processes in cellulose thermal decomposition: implications for fire-retarding strategies and treatments. Combustion Theory and Modelling, 2004. 8(2): p. 281-291.

[14] Gijsman, P., et al., Differences in the flame retardant mechanism of melamine cyanurate in polyamide 6 and polyamide 66. Polymer Degradation and Stability, 2002. 78(2): p. 219-224.

[15] Ayani, M.B., J.A. Esfahani, and R. Mehrabian, Downward flame spread over PMMA sheets in quiescent air: Experimental and theoretical studies. Fire Safety Journal, 2006. 41(2): p. 164-169.